Cognitive Overlay for Inter-system Cellular Dynamic Spectrum Sharing in the Downlink

Jared S. Everett and Brian L. Mark
Electrical and Computer Engineering Department
George Mason University
Fairfax, Virginia, United States
jared.everett@ieee.org, bmark@gmu.edu

Abstract—This paper assesses the feasibility of a novel dynamic spectrum sharing approach for a cellular downlink based on *cognitive overlay* to allow non-orthogonal cellular transmissions from a primary and a secondary radio access technology concurrently on the same radio resources. The 2-user Gaussian cognitive interference channel is used to model a downlink scenario in which the primary and secondary base stations are co-located. A system architecture is defined that addresses practical challenges associated with cognitive overlay, in particular the non-causal knowledge of the primary user message at the cognitive transmitter. A cognitive overlay scheme is applied that combines superposition coding with dirty paper coding, and a primary user protection criterion is derived that is specific to a scenario in which the primary system is 4G while the secondary system is 5G. Simulation is used to evaluate the achievable signal-to-interference-plus-noise ratio (SINR) at the 4G and 5G receivers, as well as the cognitive power allocation parameter as a function of distance. Results suggest that the cognitive overlay scheme is feasible when the distance to the 5G receiver is relatively small, even when a large majority of the secondary user transmit power is allocated to protecting the primary user transmission. Achievable link distances for the 5G receiver are on the order of hundreds of meters for an urban macrocell or a few kilometers for a rural macrocell.

Index Terms—spectrum sharing, cognitive radio, cognitive overlay, cellular, inter-system

I. INTRODUCTION

Efficient refarming of commercial spectrum is a perennial challenge that arises with the introduction of any new generation of cellular technology. In addition to providing wide geographic coverage for next generation services as rapidly as possible, network operators must retain support for legacy technologies. In the transition from 4G to 5G cellular networks, dynamic spectrum sharing (DSS) has been introduced as a new approach to allow inter-system scheduling of radio resources for both Long Term Evolution (LTE) and New Radio (NR) on a shared carrier. Although this dynamic approach is more efficient than traditional static refarming, it remains limited by the fact that resources must be shared in an orthogonal manner. As beyond 5G cellular networks become increasingly dense with the introduction of new verticals supporting massive numbers of devices, enhancements to current orthogonal DSS approaches may be required.

Cognitive radio offers an alternative toolbox of techniques that can address this problem. One widely cited taxonomy of cognitive radio paradigms defines three general approaches: *interweave*, *underlay*, and *overlay* [1]. In the cognitive overlay paradigm, a cognitive *secondary user* (SU) uses side information about the message and coding scheme of a non-cognitive *primary user* (PU) to transmit on the same channel as the PU in a non-orthogonal manner. Advanced coding and signal processing techniques are used by the SU to maintain or improve the performance of the PU.

In this paper, we assess the feasibility of a novel approach to inter-system cellular DSS that takes advantage of cognitive overlay to allow non-orthogonal transmission of two radio access technologies (RATs) on the same radio resources at the same time and frequency. This approach goes beyond currently standardized 5G capabilities. However, the concept is not limited to a specific cellular generation. It can be used for future 5G/6G DSS or added as a new feature for 4G/5G DSS in a future specification release. For the remainder of this paper, we will focus on 4G/5G DSS, though the proposed cognitive overlay approach has wider applicability.

In the context of 4G/5G DSS, the 4G network plays the role of the primary system while the 5G network is the secondary system. The scenario is constrained to the cellular downlink with the 4G LTE evolved Node B (eNB) and the 5G NR next generation Node B (gNB) co-located at a single base station (BS) site. We describe a system architecture that addresses some of the practical challenges associated with cognitive overlay techniques. We apply a cognitive overlay scheme that uses superposition coding to protect the primary LTE user, combined with dirty paper coding (DPC) to remove the adverse effects of interference on the secondary NR user. An evaluation of the signal-to-interference-plus-noise ratio (SINR) at the LTE and NR user equipment (UEs) is used to assess the feasibility of the cognitive overlay scheme and develop an upper bound on the achievable SINR at the NR UE. Performance evaluation using practical coding schemes, such as those proposed in [2], remains a topic for future study.

Prior work on applications of cognitive overlay has addressed a variety of communications scenarios involving, e.g., broadcast television networks [3]–[6], cellular networks [7]–[9], satellite networks [10]–[12], and combinations thereof. The cognitive overlay scheme used in this paper is adapted from [3] for spectrum sharing between a PU digital television (DTV) system and a SU cellular system. The application of this scheme to cellular inter-system DSS is novel. The main

differences between our model and that of [3] are the definition of a PU protection criterion and simulation parameters that are specific to the cellular inter-system downlink DSS scenario. The 3GPP cellular propagation model is also used for realism. A related application of cognitive overlay for cellular dynamic spectrum access was proposed in [7]. However, that work constrains the locations of the UEs such that the channel model can be approximated as a Z-channel [13]. As a result, superposition coding is not required, and the derivation of the cognitive overlay scheme, protection criterion, and SINR are different. In contrast, our analysis is more general and does not impose distance constraints.

The remainder of this paper is outlined as follows. Section II provides a review of the cognitive overlay approach. Section III describes the system architecture for the 4G/5G DSS scenario considered in this paper. Section IV defines the cognitive overlay transmission scheme. Section V presents numerical results based on simulation of channel propagation characteristics. Section VI provides concluding remarks.

II. CHANNEL MODEL AND CODING TECHNIQUES

A. Cognitive Interference Channel Model

The cognitive overlay paradigm is modeled using the cognitive interference channel (CIC), first introduced in a single-input, single-output (SISO) channel setting in [14] and later extended to multiple-input, multiple-output (MIMO) channels in [15]. In this paper we focus on the SISO channel model to understand the impact of large-scale propagation aspects on achievable signal power. The insights gained in the SISO analysis are also useful in understanding the MIMO case at a macroscopic level.

The contents of the blue box in Fig. 1 shows the 2-user Gaussian CIC (G-CIC) in general form [13, Appendix A], which is a special case of the 2-user discrete-time memoryless CIC (DM-CIC). Hereafter, we simply refer to this model as the G-CIC, unless another distinction is made. As in the classical interference channel model [16], two users transmit their messages over a shared channel creating mutual interference. The resulting network has four nodes: a PU transmitter and receiver (i.e., T_P and R_P) and a SU transmitter and receiver (i.e., T_S and R_S). The PU and SU messages are denoted W_P and W_S, respectively. Cognition is modeled by providing T_S with non-causal knowledge of W_P. Additionally, it is generally assumed that both transmitters have knowledge of all channel gains and codebooks [1]. However, for the scenario considered in this paper, this additional information is only required at T_S.

The received signals at R_i for $i \in \{P, S\}$ are given by the discrete time signal model

$$Y_P = h_P X_P + h_{SP} X_S + Z_P, \tag{1}$$
$$Y_S = h_S X_S + h_{PS} X_P + Z_S, \tag{2}$$

where X_i is the transmitted codeword from T_i, which satisfies the power constraint $E\{|X_i|^2\} \leq P_i$. Receiver noise, Z_i, is modeled as zero-mean complex Gaussian with variance N_i. Complex channel gains are denoted by h_P, h_S, h_{PS}, and h_{SP}.
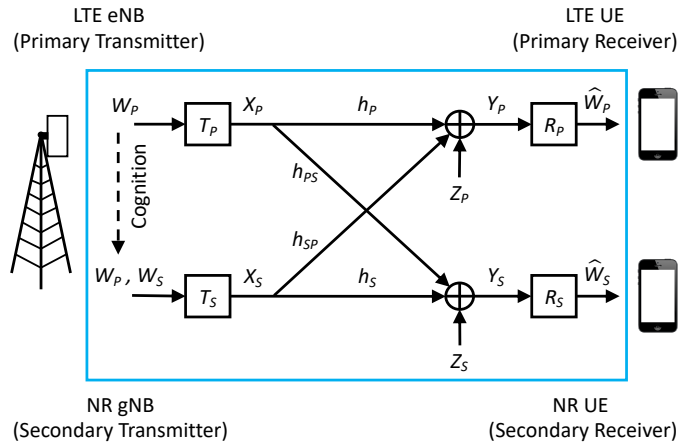

Fig. 1: The 2-user Gaussian cognitive interference channel (G-CIC) model in general form (inside blue box) and the mapping of the 4G/5G cellular DSS scenario (outside blue box).

B. Coding Techniques for the G-CIC

The G-CIC contains elements of other well-known channel models, including interference channels, broadcast channels, channels with random state, and MIMO broadcast channels. Coding techniques developed for those channels, and combinations thereof, have been investigated for the G-CIC. In this paper, we make use of the coding techniques described below. Greater detail on these techniques can be found in [16].

- **Dirty Paper Coding (DPC):** A precoding technique for single-user additive white Gaussian noise (AWGN) channels with random state known non-causally at the transmitter. DPC achieves the interference-free capacity, even when the random channel state is unknown at the receiver [17].
- **Superposition Coding:** Originally applied to the broadcast channel. The message for the weaker receiver is first encoded at a lower rate. The message for the stronger receiver is then superimposed (i.e., encoded using a correlated codebook) to form the transmitted codeword. The weaker receiver decodes the superimposed message as noise.

Practical coding schemes for the G-CIC that combine superposition coding with DPC are studied in [2] for the weak interference, very strong interference, and primary decodes cognitive regimes.

C. Non-Causal Message Knowledge

In practice, the assumption that the cognitive transmitter has non-causal knowledge of the primary transmitter's message before it is sent is problematic. Prior work on applications of cognitive overlay typically address this problem in one of two ways:

1) A scenario is devised in which the non-causal message knowledge can be provided to T_S *a priori* through some out-of-band side channel.
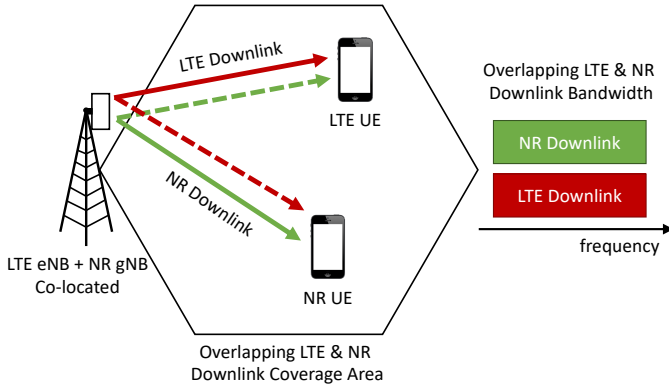
Fig. 2: System architecture for 4G/5G downlink DSS scenario.

2) A 2-phase protocol is devised whereby X_P is obtained causally in phase 1, then exploited as in the non-causal G-CIC model in phase 2.

In the present paper, we use the first approach, the details of which are described in Section III.

III. SYSTEM ARCHITECTURE

In the 4G/5G DSS scenario, a pre-existing LTE network is deployed in a given frequency band, and the network operator wishes to deploy 5G NR on the same carrier in the same geographic area using cognitive overlay. Within the cognitive radio context, the LTE portion of the network is considered to be the PU, and the NR overlay is the SU. This arrangement implies that we wish to concentrate any modifications necessary to implement the new cognitive overlay feature on the NR protocols while requiring minimal or no changes to the LTE protocols for backward compatibility.

We focus on the downlink transmission and further constrain the system to the scenario in which the LTE eNB and the NR gNB are co-located. These assumptions ensure that both the LTE and NR transmissions are time-aligned at the UEs. The co-location of the LTE eNB and the NR gNB addresses the requirement for non-causal knowledge of X_P at T_S, as discussed later in this section. This assumption is reasonable, given that many early 5G deployments will begin by adding NR coverage using existing cell sites due to the lengthy process associated with the approval of new cell sites, such as those required for massive small cell deployment.

The overall system architecture is shown in Fig. 2, which illustrates the downlink transmission from the BS to the LTE UE and NR UE. For this study, we consider a single cell environment. The solid lines between the BS and the UEs in Fig. 2 represent the transmission of the primary and secondary messages to their intended users (e.g., LTE eNB transmission to the LTE UE). The dashed lines represent interference.

To address the problem of non-causal message knowledge at T_S, we introduce the concept of information sharing between the LTE scheduler and the NR scheduler at the baseband units (BBUs). Modern cellular BSs can be divided into two components: the BBU and the radio unit (RU). The BBU

is responsible for baseband processing of the layer 1, 2, and 3 cellular protocols on the air interface. The physical layer (PHY) complex baseband symbols are carried over fiber to and from the RU located at the top of the cell tower. Hardware from a single vendor commonly supports multiple BBUs within a single BS. This configuration can be used, e.g., to support an LTE eNB and an NR gNB within a single box. In this configuration, the eNB and gNB BBUs are connected by a high-speed backplane, making it possible to share large volumes of data. We assume that the medium access control (MAC) layer scheduler in the BBU of the LTE eNB can share its scheduling information in real time with the scheduler in the BBU of the NR gNB. We leverage the co-location of the eNB and gNB, combined with an interface between the BBUs of the two systems, to provide knowledge of the LTE transmission non-causally to the NR gNB.

IV. COGNITIVE OVERLAY SCHEME

A. Cognitive Transmission Scheme

We model the 4G/5G downlink DSS scenario using the G-CIC. In this scenario, the LTE eNB is the primary transmitter (T_P), the LTE UE is the primary receiver (R_P), the NR gNB is the secondary transmitter (T_S), and the NR UE is the secondary receiver (R_S). This mapping is shown outside the blue box in Fig. 1.

The cognitive transmission scheme at T_S combines superposition coding with DPC. Secondary transmitter T_S uses part of its power to help convey W_P to R_P and the remainder of its power to convey W_S to R_S. The cognitive power allocation parameter, $\alpha \in [0, 1]$, denotes the ratio of P_S used to convey W_P. Superposition coding is used to generate the secondary transmitted codeword,

$$X_S = \sqrt{(1-\alpha)} \cdot \hat{X}_S + \sqrt{\frac{\alpha P_S}{P_P}} \cdot X_P, \qquad (3)$$

where $\hat{X}_S$ is the signal component that conveys W_S to R_S. The codebooks for each signal component are assumed to be Gaussian, i.e., $X_P \sim N(0, P_P)$, $X_S \sim N(0, P_S)$, and $\hat{X}_S \sim N(0, P_S)$. DPC is applied to $\hat{X}_S$ to mitigate interference from X_P at R_S.

B. Primary User Protection Criterion

The portion of P_S used to send $\hat{X}_S$ creates interference at R_P that is not addressed by DPC. To ensure PU performance does not degrade, a protection criterion is defined in terms of α. Applying the secondary encoding scheme, (3), to (1) yields

$$Y_P = \left(h_P + h_{SP}\sqrt{\frac{\alpha P_S}{P_P}} \right) X_P + h_{SP}\sqrt{(1-\alpha)}\hat{X}_S + Z_P.$$
$$(4)$$

The first term on the right is the combination of X_P from T_P and T_S at R_P. The remaining terms for $\hat{X}_S$ and Z_P are interference and noise, respectively. The SINR at R_P is then

$$\text{SINR}_P = \frac{\left| h_P + h_{SP}\sqrt{\frac{\alpha P_S}{P_P}} \right|^2 P_P}{N_P + (1-\alpha)|h_{SP}|^2 P_S}. \qquad (5)$$

This expression is maximized when the received signals from T_P and T_S are coherently aligned at R_P. Since we have defined the scenario such that the LTE eNB and the NR gNB are co-located, this is theoretically possible for unicast messages intended for a single LTE UE if the LTE eNB and NR gNB both have detailed channel state information (CSI). However, for this analysis we begin with the simpler case in which the signals are not coherently aligned at R_P. If we assume that the phase difference is random and uniformly distributed, the average SINR becomes

$$\overline{\text{SINR}}_P = \frac{|h_P|^2 P_P + \alpha |h_{SP}|^2 P_S}{N_P + (1-\alpha)|h_{SP}|^2 P_S}. \quad (6)$$

Next we need to derive a value for α that protects the PU from degradation due to the SU transmission. In the absence of the SU, the channel reduces to a single-user AWGN channel:

$$Y_P = h_P X_P + Z_P. \quad (7)$$

Then the single-user SNR at R_P is simply

$$\text{SNR}_P = \frac{|h_P|^2 P_P}{N_P}. \quad (8)$$

We select the conservative protection criterion that the average SINR at R_P should be equivalent to the single-user SNR at R_P if $P_S = 0$. This is equivalent to requiring the SU to do zero harm to the PU. By setting (6) equal to (8) and solving for α, we find that the protection criterion is met when

$$\alpha = \frac{|h_P|^2 P_P}{N_P + |h_P|^2 P_P}. \quad (9)$$

By this definition, α is only a function of parameters of the PU. This has two significant implications. First, the power allocation strategy at T_S is independent of the parameters of the SU (i.e., P_S, h_S, and N_S) and the cross-channel gains (i.e., h_{SP} and h_{PS}). Second, it is straightforward for T_S to acquire the necessary information to calculate α without any modifications to the LTE PHY protocol. LTE already supports feedback of CSI from the UE to the eNB. The LTE UE acquires this information by performing channel estimation on downlink reference signals (RS) (i.e., pilots). Since we have already established that the NR gNB will acquire non-causal knowledge of W_P through information sharing from the LTE eNB BBU to the NR gNB BBU, it is reasonable to assume that the CSI can be shared as well.

C. Secondary User Performance

This section establishes a simple upper bound on the SINR experienced at R_S. Applying the secondary encoding scheme (3) to (2) yields

$$Y_S = h_S \sqrt{(1-\alpha)}\hat{X}_S + \left(h_{PS} + h_S \sqrt{\frac{\alpha P_S}{P_P}} \right) X_P + Z_S. \quad (10)$$

The transmission of X_P from both T_P and T_S creates interference at R_S. In the ideal scenario, the use of DPC allows T_S to encode $\hat{X}_S$ such that the adverse effects of interference

TABLE I: System Parameters

Parameter	Scenario 1	Scenario 2
3GPP Scenario Name	Rural Macrocell	Urban Macrocell
3GPP Scenario Abbrev.	RMa	UMa
Outdoor/Indoor	Outdoor	Outdoor
Carrier Frequency (f_c)	700 MHz	1800 MHz
Nominal Bandwidth	10 MHz	10 MHz
Occupied Bandwidth	9 MHz	9 MHz
Thermal Noise (N_P, N_S)	-105 dBm	-105 dBm
LTE Transmit Power (P_P)	20 W	20 W
NR Transmit Power (P_S)	20 W	20 W
Min d_{2D} from BS to UE	35 m	35 m
Max d_{2D} from BS to UE	10 km	5 km
Height of BS (h_{BS})	35 m	25 m
Height of UE (h_{UE})	1.5 m	1.5 m
Breakpoint Distance (d_{BP})	770 m	288 m

from X_P are fully removed at R_S. This results in an upper bound on the SINR at R_S

$$\max\{\text{SINR}_S\} = \frac{(1-\alpha)|h_S|^2 P_S}{N_S}. \quad (11)$$

If we assume that the noise floor is approximately equal at R_P and R_S (i.e., $N_P = N_S = N$) and apply (9), then (11) becomes

$$\max\{\text{SINR}_S\} = \frac{|h_S|^2 P_S}{N + |h_p|^2 P_P}. \quad (12)$$

This upper bound is used in the next section to assess the feasibility of using cognitive overlay for the 4G/5G downlink DSS scenario.

V. RESULTS

A. Scenarios

Simulation is used to determine the achievable SINR at both the LTE UE and the NR UE. For realism, channel gains are determined using the most up-to-date 3GPP propagation models defined in 3GPP technical report (TR) 38.901 [18] for the evaluation of 3GPP systems for Release 14 and beyond. Two scenarios are evaluated: Rural Macrocell (RMa) and Urban Macrocell (UMa). System parameters are chosen to match the scenarios and are summarized in Table I. A nominal bandwidth of 10 MHz and BS transmit power of 20 W are used for both scenarios to facilitate comparison.

B. Propagation Model

The following large-scale propagation parameters are simulated: line-of-sight (LOS) probability, path loss, and shadow fading. The fast fading model is beyond the scope of this analysis and is not implemented. The ground distance from the BS to the UE is denoted d_{2D}, and the slant distance accounting for antenna height is denoted d_{3D}.

Channel gains are simulated as follows. First, a scenario is selected (i.e., RMa or UMa). Second, the propagation condition is assigned as LOS or NLOS using the LOS probability defined in Table II [18, Table 7.4.2-1]. Third, the path loss is calculated according to Table 7.4.1-1 of [18]. The equations for the UMa scenario are shown in Table III as an example. For a given LOS condition, path loss is a deterministic function of

TABLE II: LOS Probability for 3GPP Propagation Model

Scenario	LOS Probability
RMa	$\Pr_{\text{LOS}} = \begin{cases} 1, & d_{\text{2D}} \leq 10 \text{ m} \\ e^{\left(\frac{-d_{\text{2D}}-10}{1000}\right)}, & d_{\text{2D}} > 10 \text{ m} \end{cases}$
UMa	$\Pr_{\text{LOS}} = \begin{cases} 1, & d_{\text{2D}} \leq 18 \text{ m} \\ \frac{18}{d_{\text{2D}}} + \left(1 - \frac{18}{d_{\text{2D}}}\right) e^{\left(\frac{-d_{\text{2D}}}{63}\right)}, & d_{\text{2D}} > 18 \text{ m} \end{cases}$

(a) RMa scenario

(b) UMa scenario

Fig. 3: Cognitive power allocation parameter (α) vs. distance to LTE UE (d_{LTE}).
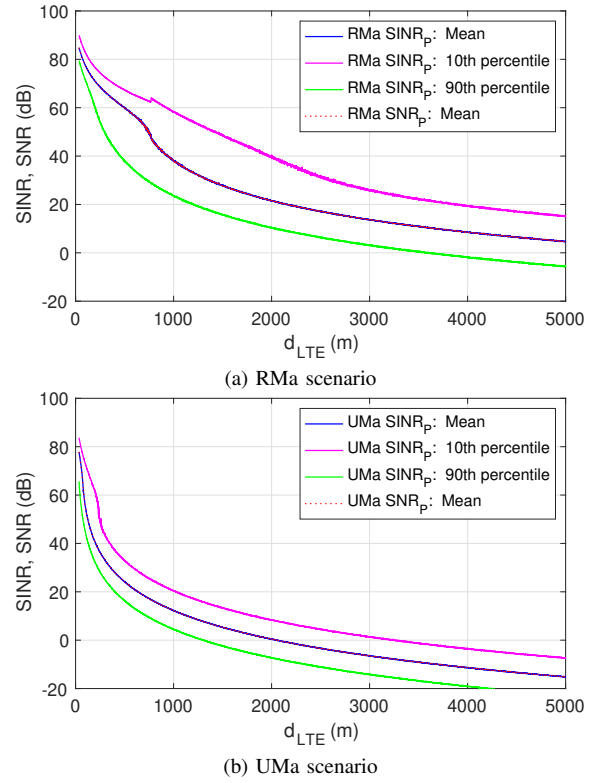

(a) RMa scenario

(b) UMa scenario
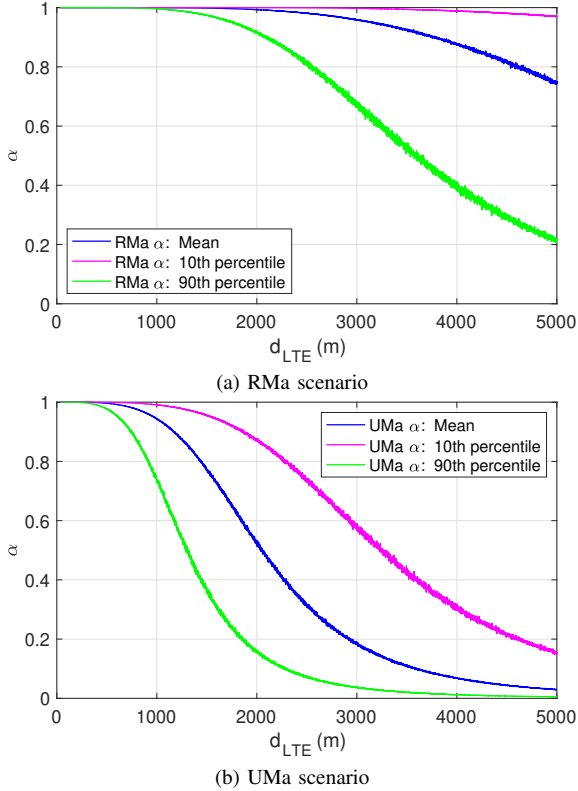
Fig. 4: Average LTE UE SINR ($\overline{\text{SINR}}_P$) and single-user SNR (SNR_P) vs. distance to LTE UE (d_{LTE}).

d_{2D}, f_c, h_{BS}, and h_{UE}. Fourth, the shadow fading is calculated using a log-normal distribution with standard deviation defined in Table 7.4.1-1 of [18]. Values for the UMa scenario are again shown in Table III as an example. Finally, the channel gains are calculated in decibels as the additive inverse of the sum of the path loss and shadow fading. Simulation results are presented for 10,000 Monte Carlo runs.

C. Performance Analysis

Fig. 3 shows the cognitive power allocation parameter, α, as a function of d_{2D} from the BS to the LTE UE. We denote this distance as d_{LTE}. Since the channel gain is defined by a distribution, the 10th percentile, mean, and 90th percentile are shown. Since the PU received signal strength (i.e., $|h_P|^2 P_P$) tends to decrease as a function of d_{LTE}, α also tends to decrease as a function of d_{LTE} according to (9). Therefore, when d_{LTE} is small, T_S allocates most of its power to X_P. When d_{LTE} is large, T_S can allocate more of its power to $\hat{X}_S$.

Fig. 4 shows $\overline{\text{SINR}}_P$ at the LTE UE as a function of d_{LTE} according to (6). The single-user SNR at the LTE UE (i.e., SNR_P) for the mean channel gain is plotted for comparison (dotted red line). This function matches the plot of $\overline{\text{SINR}}_P$ for the mean channel gain (solid blue line), which demonstrates that the protection criterion is met (i.e., $\overline{\text{SINR}}_P = \text{SNR}_P$). This result demonstrates that the use of superposition coding at the NR gNB to protect LTE performance is feasible.

Fig. 5 shows $\max\{\text{SINR}_S\}$ at the NR UE as a function of d_{2D} from the BS to the NR UE. We denote this distance as d_{NR}. Results for three values of α are compared. For legibility, only mean channel gains are shown. Results show that the cognitive overlay scheme is feasible when d_{NR} is small. Assuming a minimum SINR of 10 dB, achievable link distances for the NR UE are on the order of hundreds of meters for UMa or a few kilometers for RMa. Surprisingly, practical NR link distances are achievable even when α equals 0.99, meaning only 1% of the gNB transmit power is allocated to sending $\hat{X}_S$ to the NR UE. Therefore, this approach may be possible even when d_{LTE} is small, although NR performance will be reduced. These results represent an upper bound on SINR_S assuming ideal performance of the DPC scheme.

VI. CONCLUSION

This paper investigated the novel application of cognitive overlay to an inter-system cellular DSS scenario in the down-link, using 4G/5G DSS as an example. Simulation results of

TABLE III: Example Pathloss and Shadow Fading for 3GPP Propagation Model Urban Macrocell Scenario

Scenario	LOS	Pathloss (dB)[a]	Shadow Fading Std. Dev. (dB)
UMa	LOS	$PL_{\text{UMa-LOS}} = \begin{cases} PL_1, & 10 \text{ m} \leq d_{\text{2D}} < d_{BP} \\ PL_2, & d_{BP} \leq d_{\text{2D}} \leq 5 \text{ km} \end{cases}$ $PL_1 = 28 + 22\log_{10}(d_{\text{3D}}) + 20\log_{10}(f_c)$ $PL_2 = 28 + 40\log_{10}(d_{\text{3D}}) + 20\log_{10}(f_c) - 9\log_{10}((d_{BP})^2 + (h_{BS} - h_{UE})^2)$	$\sigma_{\text{SF}} = 4$
	NLOS	$PL_{\text{UMa-NLOS}} = \max\{PL_{\text{UMa-LOS}}, PL'_{\text{UMa-NLOS}}\}, 10 \text{ m} \leq d_{\text{2D}} \leq 5 \text{ km}$ $PL'_{\text{UMa-NLOS}} = 13.54 + 39.08\log_{10}(d_{\text{3D}}) + 20\log_{10}(f_c) - 0.6(h_{UE} - 1.5)$	$\sigma_{\text{SF}} = 6$

[a]Carrier frequency (f_c) is in GHz. Distances $(d_{\text{2D}}, d_{\text{3D}}, d_{BP})$ are in meters.

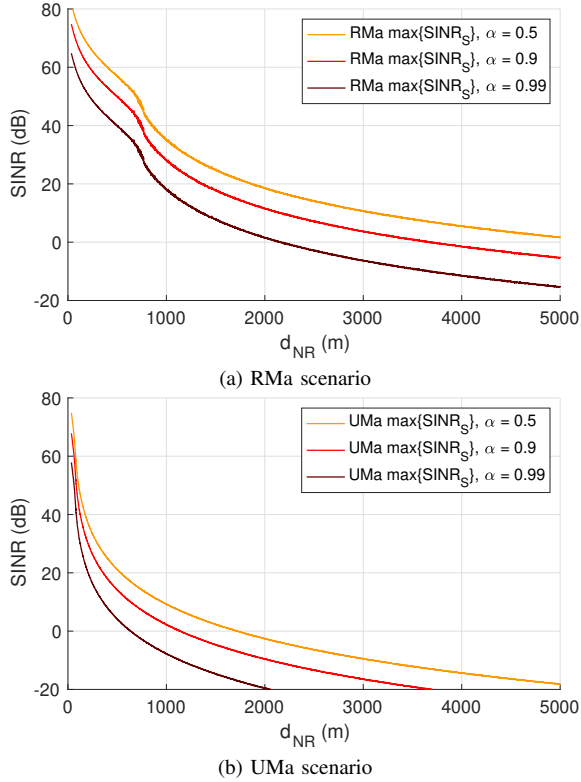

(a) RMa scenario

(b) UMa scenario

Fig. 5: Upper bound on NR UE SINR ($\max\{\text{SINR}_S\}$) vs. distance to NR UE (d_{NR}) for different values of cognitive power allocation parameter (α) and mean channel gains.

SINR at the 4G and 5G receivers suggest that this scheme is feasible, and SU performance increases when the secondary NR UE is closer to the BS and the primary LTE UE is further from the BS. In ongoing work, we are extending our analysis to the multiple-input, multiple-output (MIMO) CIC setting based on the channel model defined in [15]. The next step is to implement practical DPC coding schemes, e.g., [2], [19], in the proposed inter-system cognitive overlay scheme and assess performance against the upper bound defined by (11) and (12).

REFERENCES

[1] A. Goldsmith, S. A. Jafar, I. Maric, and S. Srinivasa, "Breaking spectrum gridlock with cognitive radios: An information theoretic perspective," *Proc. IEEE*, vol. 97, no. 5, pp. 894–914, 2009.
[2] E. Kurniawan, A. Goldsmith, and S. Rini, "Practical coding schemes for cognitive overlay radios," in *IEEE GLOBECOM*, 2012.
[3] J. Sachs, I. Maric, and A. Goldsmith, "Cognitive cellular systems within the TV spectrum," in *IEEE DySPAN*, 2010.
[4] Y. Selen, R. Baldemair, and J. Sachs, "A short feasibility study on a cognitive TV black space system," in *IEEE 22nd Int. Symp. Personal, Indoor and Mobile Radio Comm.*, 2011.
[5] S. Sun, Y. Ju, and Y. Yamao, "Overlay cognitive radio OFDM system for 4G cellular networks," *IEEE Wireless Commun. Mag.*, vol. 20, no. 2, pp. 68–73, Apr. 2013.
[6] Y. Beyene, K. Ruttik, and R. Jantti, "Effect of secondary transmission on primary pilot carriers in overlay cognitive radios," in *Int. Conf. Cognitive Radio Oriented Wireless Networks Comm. (CROWNCOM)*, 2013.
[7] A. S. Alam, L. S. Dooley, and A. S. Poulton, "Dynamic spectrum access based on cognitive radio within cellular networks," in *Wireless Advanced (WiAd)*, 2011.
[8] M. Maso, L. S. Cardoso, M. Debbah, and L. Vangelista, "Cognitive orthogonal precoder for two-tiered networks deployment," *IEEE J. Sel. Areas Commun.*, vol. 31, no. 11, pp. 2338–2348, Nov. 2013.
[9] A. Abdou, A. Abdo, and A. Jamoos, "Overlay cognitive radio based on OFDM with channel estimation issues," *Wireless Personal Comm.*, vol. 108, no. 2, pp. 1079–1096, Sep. 2019.
[10] S. K. Sharma, S. Chatzinotas, and B. Ottersten, "Satellite cognitive communications: Interference modeling and techniques selection," in *6th Adv. Satellite Multimedia Sys. Conf. (ASMS) and 12th Signal Proc. for Space Comm. Workshop (SPSC)*, 2012.
[11] R. P. Sirigina, A. S. Madhukumar, and M. Bowyer, "NOMA precoding for cognitive overlay dual satellite systems," in *IEEE Veh. Tech. Conf. (VTC)*, 2019.
[12] L. B. C. da Silva, T. Benaddi, and L. Franck, "On the feasibility of a secondary service transmission over an existent satellite infrastructure: design and analysis," *EURASIP J. Wireless Comm. and Netw.*, Mar. 2020.
[13] S. Rini, D. Tuninetti, and N. Devroye, "Inner and outer bounds for the Gaussian cognitive interference channel and new capacity results," *IEEE Trans. Inf. Theory*, vol. 58, no. 2, pp. 820–848, Feb. 2012.
[14] N. Devroye, P. Mitran, and V. Tarokh, "Achievable rates in cognitive radio channels," *IEEE Trans. Inf. Theory*, vol. 52, no. 5, pp. 1813–1827, 2006.
[15] S. Sridharan and S. Vishwanath, "On the capacity of a class of MIMO cognitive radios," *IEEE J. Sel. Topics in Signal Process.*, vol. 2, no. 1, pp. 103–117, Feb. 2008.
[16] A. El Gamal and Y. Kim, *Network Information Theory*. Cambridge, UK: Cambridge University Press, 2012.
[17] M. Costa, "Writing on dirty paper (corresp.)," *IEEE Trans. Inf. Theory*, vol. 29, no. 3, pp. 439–441, May 1983.
[18] 3GPP TR 38.901, "Study on channel model for frequencies from 0.5 to 100 GHz," Release 16, ver. 16.1.0, 2019.
[19] K. Rege, K. Balachandran, J. Kang, and M. Karakayali, "Practical dirty paper coding with sum codes," *IEEE Trans. Commun.*, vol. 64, no. 2, pp. 441–455, Feb. 2016.